Self-accelerating and self-breathing Bessel-like beams along arbitrary trajectories

Juanying Zhao (赵娟莹)[1,2], Peng Zhang (张 鹏)[2,3], Dongmei Deng (邓冬梅)[2,4], Cibo Lou (楼慈波)[5], Daohong Song (宋道红)[5], Jingjiao Liu (刘京郊)[1], and Zhigang Chen (陈志刚)[2,5*]

[1] *School of Optoelectronics, Beijing Institute of Technology, Beijing 100081, China*

[2] *Department of Physics and Astronomy, San Francisco State University, San Francisco, CA 94132, USA*

[3] *NSF Nanoscale Science and Engineering Center, University of California, Berkeley, CA 94720, USA*

[4] *Laboratory of Nanophotonic Functional Materials and Devices, South China Normal University, Guangzhou 510631, China*

[5] *The MOE Key Laboratory of Weak Light Nonlinear Photonics and TEDA Applied Physics School, Nankai University, Tianjin 300457, China*

[*] *Corresponding author: zhigang@sfsu.edu*

Received July 23, 2013; accepted September 16, 2013; posted online November 6, 2013

We theoretically and experimentally study self-accelerating and self-breathing Bessel-like beams that follow arbitrary trajectories, including hyperbolic, hyperbolic secant, and three-dimensional (3D) spiraling trajectories. The beams have an overall Bessel-like profile in transverse dimensions; however, the intensity of their central main lobe breathes while traveling along a curved trajectory. Such beams can be readily generated experimentally through appropriate phase modulation of the optical wavefront. The beams contribute to the design of new families of self-accelerating beams.

OCIS codes: 070.7345, 070.6120, 070.2580, 090.1760.

doi: 10.3788/COL201311.110701.

Optical beams along curved trajectories have been of particular interest since self-accelerating (self-bending) Airy beams were first proposed and observed several years ago by Christodoulides' group[1,2]. A general method of finding self-accelerating beams is to obtain exact solutions from either the Maxwell equations or the time-independent Helmholtz equations. For example, nondiffracting, circular, accelerating wave packets of Maxwell's equations were previously predicted and demonstrated as typical large-angle, nonparaxial accelerating beams[3−5]. Soon after, nonparaxial Mathieu and Weber beams were proposed and proven; these beams suggest that accelerating beams can be generalized to elliptic and parabolic trajectories[6−8]. Various approaches have been developed in paraxial regimes for generating accelerating beams along curved trajectories. For instance, a snake-like beam with paraxial arbitrary focal lines was created by a computer-generated hologram[9]. Spiraling zero-order Bessel beams traveling around a straight line have also been designed and analyzed[10]. Bessel-like beams, which feature a symmetric and nonspreading central main lobe, accelerating along arbitrary curved trajectories were recently proposed and demonstrated by specially designed optical wavefront phase modulation[11,12]. Self-bending beams along the zigzag or periodic trajectories have also been proposed[13] and observed[14,15].

In the current study, we generate self-breathing accelerating optical beams propagating along arbitrary trajectories based on our previous work on Bessel-like accelerating beams[11,12]. Examples of trajectories include the hyperbolic, hyperbolic secant, and three-dimensional (3D) spiraling trajectories. These beams can be obtained by engineering the phase of a Gaussian beam, following the same approach of phase modulation developed by Chremmos *et al.*[11] for generating accelerating Bessel-like beams. Specifically, the beams feature an annulus phase on their input plane, so that conical bundles of rays with apexes that write a focal curve with pre-specified shapes are formed. In the present study, by removing the phase annulus alternatively (i.e., adding effective amplitude modulation), the intensity of the resulting main lobe of the Bessel-like beam exhibits a breathing or pulsating feature as the intensity peak location alternately changes between the main lobe and the outer rings during propagation. Such self-breathing and self-accelerating beams are of fundamental interest and may be utilized in practical applications.

Firstly, we simulate the propagation of a breathing self-accelerating Bessel-like beam using the theoretical model proposed in Ref. [11]. The complex amplitude of the light field $u(x, y, z)$, which propagates along the z-axis in the Cartesian coordinate, is governed by the Fresnel integral:

$$u(x,y,z)=\frac{1}{2\pi \mathrm{i}z}\iint u(x_0,y_0,0)\mathrm{e}^{\mathrm{i}\frac{(x-x_0)^2+(y-y_0)^2}{2z}}\mathrm{d}x_0\mathrm{d}y_0, \tag{1}$$

where $u(x_0,y_0,0)=\exp[-(x_0^2+y_0^2)/w^2]\exp[\mathrm{i}Q1(x_0,y_0)]$ is the initial complex amplitude distribution of the optical field, w is the characteristic beam size, and $Q1$ is the modified phase modulation from a specially designed Q function[11], which can be obtained from

$$Q(x,y)=\frac{k_0}{2}\int_0^z\{[f'(\zeta)]^2+[g'(\zeta)]^2-(\beta/k_0)^2\}\mathrm{d}\zeta - k_0\frac{(f-x)^2+(g-y)^2}{2z}, \tag{2a}$$

$$\beta^2z^2/k_0^2=[x-f(z)+zf'(z)]^2+[y-g(z)+zg'(z)]^2, \tag{2b}$$

where k_0 is the free space wavenumber; β is the transverse normalized coefficient; $[f(z), g(z)]$ is the predesigned trajectory; $f'(z)$ and $g'(z)$ are the derivatives of $f(z)$ and $g(z)$ versus z, respectively; ζ is the variable. In the above equations, $z(x, y)$ consists of a series of expanding circles with a moving center $[f(z)-zf'(z), g(z)-zg'(z)]$, as shown in Fig. 1. In addition, Q is constituted by a series of smoothly continuous isocurves. $Q1$ results from Q binarization, which is defined by

$$Q1=\begin{cases} 0 & \min\_Q \leqslant Q < \min\_Q + c \\ 1 & \min\_Q + c \leqslant Q < \min\_Q + 2c \\ 0 & \min\_Q + 2c \leqslant Q < \min\_Q + 3c \\ 1 & \min\_Q + 3c \leqslant Q < \min\_Q + 4c \\ \vdots & \vdots \\ \begin{cases} 0 & 2[n/2] = n \\ 1 & 2[n/2] \neq n \end{cases} & \min\_Q + nc \leqslant Q \leqslant \max\_Q \end{cases}, \tag{3}$$

where max_Q and min_Q are the maximum and minimum values, respectively, of Q; c is a constant that satisfies the criteria $0< c <(\max\_Q\text{-}\min\_Q)/2$; the parameter $n = [\max\_Q/c]$ is the maximum integer of $\max\_Q/c$ (fractions are rounded down); $n+1$ is the number of the annulus.

We readily obtain $Q1$ from the following equations in our Matlab code.

$$Q' = Q - 2c\left[\frac{Q}{2c}\right], \tag{4a}$$

$$Q1 = \begin{cases} 1 & Q' \geqslant c \\ 0 & Q' < c. \end{cases} \tag{4b}$$

For example, we show a phase Q in Fig. 2(a), which smoothly decreases along the radial direction. Afterward, we divide Q into a series of "period" rings Q' (Fig. 2(b)), which is the remainder of Q when divided by $2c$ ($c=\pi$). In this example, the "period" $2c$ is the modulated width ΔQ for every ring. The values of the period (between 0 and $2c$) along the white dotted line are shown in Fig. 2(d). Finally, a "well"-shaped phase $Q1$ (Fig. 2(c)) is obtained from Q' by Eq. (4b). As shown in Fig. 2(d), the values along the dotted line are 1 and 0 on the red and blue rings, respectively. This approach yields the new phase $Q1$. In the phase $Q1$, the beams

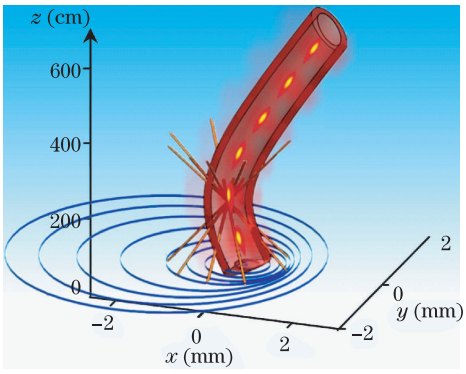

Fig. 1. (Color online) Schematic of the principle. Rays emitted from expanding circles $z(x,y)$ on the input plane intersect on the specified focal curve. Circles are removed alternatively so that the main lobe breathes during propagation.

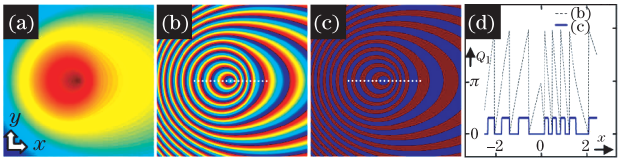

Fig. 2. (Color online) Theoretical analysis of the phase $Q1$. (a) Original phase Q obtained from Eq. 2, (b) phase Q', (c) phase $Q1$, and (d) value of phases $Q1$ and Q' along the white line in (b) and (c).

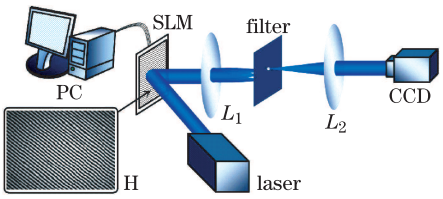

Fig. 3. (Color online) Schematic of the experimental setup for generating self-accelerating breathing optical beams via computer generated holography. SLM: spatial light modulator; H: computer generated hologram; L: lens; CCD: charge-coupled device.

created in $z>0$ possess breathing transverse Bessel-like field patterns along a desired trajectory function $[f(z), g(z), z]$ in free space.

An intuitive picture of our method is illustrated in Fig. 1. Any point along the focal line represents the center of the beam, as constructed from the conical ray bundles emitted from the expanding circle $z(x, y)$ on the input plane. The transverse beam profile takes a form close to the Bessel function $J_0(r)$. The "periodically" modulated phase $Q1$ suggests that these expanding circles are divided into intermittent annuli. The alternate disappearing main lobe results from the intermittently "removed" annuli. In addition, the breathing trajectory interval is determined by the annular width Δz on the input plane. The intensity peak location alternately changes between the main lobe and the outer rings of the Bessel-like beam.

To experimentally demonstrate the breathing accelerating beams, we illuminate a phase-only spatial light modulator (SLM) with a plane wave. The SLM is programmed by a hologram[16] with the desired phase profile, which is obtained by computing the interference between initial optical field $u(x_0, y_0, 0)$ and a tilted plane wave, as depicted in Fig. 3. Upon reflection from the hologram, the coded phase information is reconstructed via a spatial filtering $4f$ system. Afterward, we record the transverse intensity patterns of the breathing accelerating beams using a charge-coupled device (CCD) camera at different propagation distances.

For the hyperbolic trajectory, the initial field is the modulated Gaussian beam ($w=30$) determined by the binary phase ($c=\pi/2$) shown in Fig. 4(a). Numerical results of breathing beam propagation along a hyperbolic trajectory are shown in Fig. 4(b). Figure 4(b) shows that the breathing beam propagates along the hyperbolic trajectory. For a propagation distance of 200 cm, nine quasi-periodic breaths are noted in the main lobe of the beam. The quasi-period of the breath can be controlled with ease by adjusting the modulated width

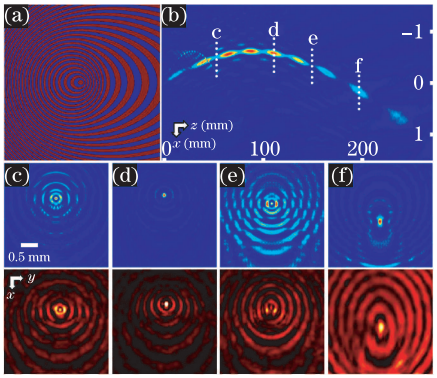

Fig. 4. (Color online) Numerical and experimental demonstrations of a self-accelerating breathing beam along a hyperbolic trajectory. (a) Binary modulated input phase for the optical breathing beam with $f(z) = \sqrt{7.5\times10^{-7}z^2-2.6\times10^{-4}z+0.05}-\sqrt{0.05}$, $g(z)=0$; (b) numerically simulated side-view propagation of the generated beam; (c)–(f) numerical (second row) and experimental (bottom row) snapshots of the transverse intensity patterns taken at planes marked by the dashed lines in (b).

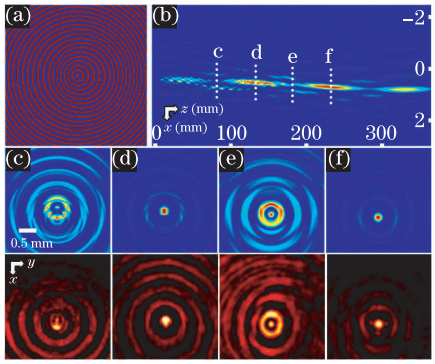

Fig. 5. (Color online) Numerical and experimental demonstrations of a self-accelerating breathing beam along a hyperbolic secant trajectory $f(z)$=0.06sech[0.007(z-315)], $g(z)$=0. (a) Binary modulated input phase; (b) numerically simulated side-view propagation of the generated beam. (c)–(f) numerical (middle row) and experimental (bottom row) snapshots of the transverse intensity patterns taken at planes marked by the dashed lines (b).

c of the rings in the phase function $Q1$ (Fig. 4(a)). Transverse intensity patterns obtained at different z are shown in Figs. 4(c)–(f); these figures clearly illustrate that the beams possess a Bessel-like intensity profile. The main lobe appears and disappears alternately during propagation as the intensity peak location changes between the central lobe and outer rings of the Bessel-like beam alternately during propagation. The experimental transverse patterns, which are obtained by employing the hologram shown in Fig. 3, are shown in the bottom row. Good agreement between the experimental results and our theoretical prediction is observed.

By following a similar procedure, we demonstrate that breathing Bessel-like beams propagate along a hyperbolic secant trajectory, as presented in Fig. 5. The binary phase with the modulated width $c=\pi$ is shown in Fig. 5(a), and the direct side view of the breathing hyperbolic secant beam is shown in Fig. 5(b). The main lobe obviously breathes along the trajectory, and the beam exhibits an intermittent pattern while propagating along the hyperbolic secant trajectory. Compared with a Gaussian beam (not shown here), the measured transverse breathing main lobe of these beams shows no diffraction during the entire course of propagation. Again, the experimental results agree well with the numerical results.

We further illustrate that self-accelerating breathing beams can follow a 3D trajectory in free space. A typical trajectory is shown in Fig. 6; for this case, we have $f(z)$=0.04tanh[0.02(z-70)]+0.04 (in the $x-z$ plane) and $g(z)$=0.046sech[0.02(z-70)] (in the $y-z$ plane). The modulated period of the phase is 2π. The experimental results match those from theory with the predesigned trajectory. Figure 6(a) indicates clearly that the beam bends in both x and y directions. In addition, the intensity peak location alternately changes between the main lobe and the outer rings along the propagation direction.

Figures 7(a) and (b) show the corresponding intensity distributions of self-accelerating Bessel-like beams along the hyperbolic (Fig. 4) and hyperbolic secant (Fig. 5) trajectories, respectively. By analyzing the central intensity variation of these beams, the breathing intervals are observed to slightly differ, especially for the beam propagating along a hyperbolic trajectory (Fig. 7(a)). The center point of the beam on the trajectory is constructed from conical ray bundles emitted from the corresponding annulus. The non-periodic breathing trajectory may be caused by variations in the annular width Δz on the input plane. Based on this analysis, self-accelerating and periodically breathing beams may be generated by applying a periodic binary $z(x,y)$ as an amplitude modulator on Bessel-like beams. We leave these issues for future studies.

In conclusion, we theoretically design and experimentally demonstrate the propagation of self-accelerating and self-breathing Bessel-like beams along hyperbolic, hyperbolic secant, and 3D trajectories. The reconfigurable pulsating trajectories, combined with the nondiffracting and self-healing features of accelerating beams, may be particularly useful in various applications, such as optical trapping and particle manipulation[17−21]. Our results present novel designs of exotic optical beams, which may contribute new features and activities to the subject area of self-accelerating beams[22].

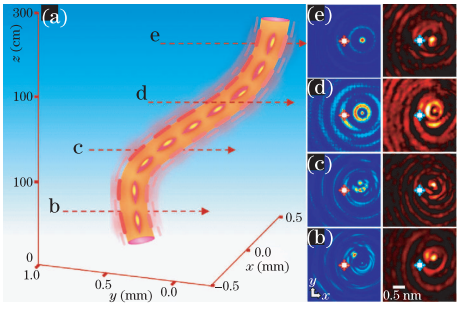

Fig. 6. (Color online) Numerical and experimental demonstration of a self-accelerating breathing beam along a 3D curved trajectory. (a) Schematic of the predesigned breathing beam along the 3D trajectory; (b–e) numerical (left column) and experimental (right column) transverse patterns taken at different marked positions in (a), where the cross marks the center of the reference non-accelerating Gaussian beam.

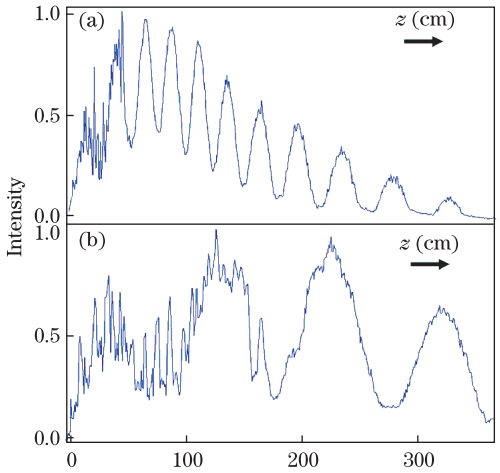

Fig. 7. (Color online) Intensity distribution of self-accelerating breathing beam along hyperbolic and hyperbolic secant trajectories. (a) Intensity variation of self-accelerating breathing beam along hyperbolic trajectory; (b) intensity variation of self-accelerating breathing beam along hyperbolic secant trajectory.

This work was supported by the National Science Foundation (NSF), the Air Force Office of Scientific Research (AFOSR), the China Scholarship Council, the National "973" Project of China (No. 2013CB632703), the NCET-10-0507, the National Natural Science Foundation of China (Nos. 11374108 and 10904041), the Foundation for the Author of Guangdong Province Excellent Doctoral Dissertation (No. SYBZZXM201227), and the Foundation of Cultivating Outstanding Young Scholars ("Thousand, Hundred, Ten" Program) of Guangdong Province in China. We express gratitude to N. K. Efremidis and D. N. Christodoulides for all of their discussions and assistance.

References

1. G. A. Siviloglou and D. N. Christodoulides, Opt. Lett. **32,** 979 (2007).
2. G. A. Siviloglou, J. Broky, A. Dogariu, and D. N. Christodoulides, Phys. Rev. Lett. **99,** 213901 (2007).
3. I. Kaminer, R. Bekenstein, J. Nemirovsky, and M. Segev, Phys. Rev. Lett. **108,** 163901 (2012).
4. P. Zhang, Y. Hu, D. Cannan, A. Salandrino, T. Li, R. Morandotti, X. Zhang, and Z. Chen, Opt. Lett. **37,** 2820 (2012).
5. F. Courvoisier, A. Mathis, L. Froehly, R. Giust, L. Furfaro, P. A. Lacourt, M. Jacquot, and J. M. Dudley, Opt. Lett. **37,** 1736 (2012).
6. P. Zhang, Y. Hu, T. Li, D. Cannan, X. Yin, R. Morandotti, Z. Chen, and X. Zhang, Phys. Rev. Lett. **109,** 193901 (2012).
7. P. Aleahmad, M. A. Miri, M. S. Mills, I. Kaminer, M. Segev, and D. N. Christodoulides, Phys. Rev. Lett. **109,** 203902 (2012).
8. M. A. Bandres and B. M. Rodriguez-Lara, New J. Phys. **15,** 013054 (2013).
9. J. Rosen and A. Yariv, Opt. Lett. **20,** 2042 (1995).
10. V. Jarutis, A. Matijosius, P. Di Trapani, and A. Piskarskas, Opt. Lett. **34,** 2129 (2009).
11. I. D. Chremmos, Z. Chen, D. N. Christodoulides, and N. K. Efremidis, Opt. Lett. **37,** 5003 (2012).
12. J. Zhao, P. Zhang, D. Deng, J. Liu, Y. Gao, I. D. Chremmos, N. K. Efremidis, D. N. Christodoulides, and Z. Chen, Opt. Lett. **38,** 498 (2013).
13. E. Greenfield, I. Kaminer, and M. Segev, in *Proceedings of Frontiers in Optics 2012/Laser Science XXVIII* FW1A.2. (2012).
14. A. Mathis, F. Courvoisier, R. Giust, L. Furfaro, M. Jacquot, L. Froehly, and J. M. Dudley, Opt. Lett. **38,** 2218 (2013).
15. Y. Hu, D. Bongiovanni, Z. Chen, and R. Morandotti, Opt. Lett. **38,** 3387 (2013).
16. T. Yamaguchi and H. Yoshikawa, Chin. Opt. Lett. **9,** 120006 (2011).
17. T. Tao, J. Li, Q. Long, and X. Wu, Chin. Opt. Lett. **9,** 120010 (2011).
18. J. Bu, G. Yuan, Y. Sun, S. Zhu, and X. Yuan, Chin. Opt. Lett. **9,** 061202 (2011).
19. J. Baumgartl, M. Mazilu, and K. Dholakia, Nature Photon. **2,** 675 (2008).
20. P. Zhang, J. Prakash, Z. Zhang, M. S. Mills, N. K. Efremidis, D. N. Christodoulides, and Z. Chen, Opt. Lett. **36,** 2883 (2011).
21. Z. Zhang, P. Zhang, M. Matthew, Z. Chen, D. N. Christodoulides, and J. Liu, Chin. Opt. Lett. **11,** 033502 (2013).
22. Y. Hu, G. A. Siviloglou, P. Zhang, N. K. Efremidis, D. N. Christodoulides, and Z. Chen, *Nonlinear Photonics and Novel Optical Phenomena* (Springer, New York, 2012).